Accepted Manuscript

Model for electrical conductivity of muscle meat during Ohmic heating

R.G.M. van der Sman

PII: S0260-8774(17)30131-0

DOI: 10.1016/j.jfoodeng.2017.03.029

Reference: JFOE 8833

To appear in: *Journal of Food Engineering*

Received Date: 10 October 2016

Revised Date: 18 February 2017

Accepted Date: 29 March 2017

Please cite this article as: van der Sman, R.G.M., Model for electrical conductivity of muscle meat during Ohmic heating, *Journal of Food Engineering* (2017), doi: 10.1016/j.jfoodeng.2017.03.029.

Model for electrical conductivity of muscle meat during Ohmic heating

R.G.M. van der Sman

Wageningen Food & Biobased Research
Wageningen University & Research

Abstract

A model is presented for predicting the electrical conductivity of muscle meat, which can be used for the evaluation of Ohmic heating. The model computes the conductivity as a function of composition, temperature and microstructure. The muscle meat is thought to be composed of protein, water, salt. Concerning the microstructure, the model takes into account the muscle fiber orientation with respect to the electric field, and the development of drip channels due to protein denaturation. The model includes a description of the protein denaturation kinetics. The model has been validated for different types of meat, varying in composition and heating rate. The submodel for protein denaturation is validated using independent DSC measurements. For meats heated faster than 20 degrees per minute, the conductivity is a linear function of temperature - due to the absence of protein denaturation, and thus drip channel formation. If meat is heated slower than 10 degrees per minute the conductivity is showing non-linear behaviour, with a significant decrease at temperatures above 70 degrees Celsius. This decrease is explained by the action of the complete protein denaturation. Our study

Email address: rugd.vandersman@wur.nl (R.G.M. van der Sman)

shows that if Ohmic heating of meat is performed at fast rates, there is a large potential to retain most of its moisture during heating.

Keywords: Electrical conductivity, protein denaturation, Ohmic heating

1. Introduction

Ohmic heating of meat is a promising technique compared to conventional cooking as it is considerably fast (Yildiz-Turp et al., 2013). Consequently, it is better in retaining water within the meat (Lyng et al., 2013). This is believed to be due to the fact that heating times are significantly shorter than that of protein denaturation. However, the Ohmic heating method can be impaired by uneven heating, which makes it difficult to determine the point with lowest temperature and thus the microbial safety (Marra, 2014; Jaeger et al., 2016). This holds particularly for composite foods having components with starkly varying electrical conductivity. Prediction of these phenomena can be improved by numerical modelling (McKenna et al., 2006; Varghese et al., 2014; Marra, 2014).

The greatest hurdle for predictive numerical modelling of Ohmic heating is the lack of knowledge on the electrical conductivity of food (Varghese et al., 2014; Kaur and Singh, 2016). Meat is particularly challenging, as the composition and structure change during heating (Oroszvári et al., 2006; Pearce et al., 2011; Bouhrara et al., 2011; Kondjoyan et al., 2013). The change in microstructure and composition is due to meat proteins denaturation. These changes influence the conductivity to a large extent (Bircan et al., 2001; Bircan and Barringer, 2002; Brunton et al., 2006; Damez and Clerjon,

2013). Furthermore, it is shown that there is a significant dependence of the conductivity on the muscle fiber direction (Zell et al., 2009).

In order to resolve this research question, we have constructed a predictive model for the electrical conductivity of meat, as function of composition, temperature and the degree of protein denaturation. Muscle meat will be viewed as a (structured) mixture of water, salt, and proteins. Regarding electrical conductivity, we will assume proteins as insulators. For salt solutions we will determine how their electrical conductivity depends on temperature and concentration, via fitting an analytical function to literature data. The conductivity of salt is mainly determined by its diffusion coefficient, or rather its mobility. The mobility of salt is hindered by the presence of the dense protein matrix in meat. This effect will be introduced via a hindrance factor. The effect of the microstructure of meat, the aligned protein fibers in the intracellular phase and the drip channels in the extracellular phase will be taken into account. The formation of drip channels is driven by protein denaturation. We account for the evolution of microstructure via modelling of the protein denaturation kinetics, and linking the state of the denatured proteins to particular microstructure. The protein denaturation submodel will be validated using independent literature data. Via combining various submodels, we compare numerical predictions with literature data on the electrical conductivity of muscle meat and meat batters, as function of temperature and heating rate.

2. Theory

2.1. Assumptions

We will regard meat as a hierarchical composite material. A composite material has a distinct dispersed phase, embedded in a continuous phase. Often the dispersed and the continuous phase differ significantly in material properties, such as electrical conductivity. During cooking meat has a composite character at two different length scales. At the larger length scale, we distinguish the extracellular and intracellular phase. The extracellular phase is filled with serum, a mixture of water, salt and soluble proteins, which has been expelled from the intracellular phase during cooking. The intracellular phase contains the muscle fibers, which are viewed as a composite material of protein fibers and serum. The electrical conductivity of the intracellular phase is considerable lower than that of the extracellular phase, due to the high volume fraction of proteins in the intracellular phase, and the steric hindrance they impose on the ion mobility.

The intracellular phase is bounded by collageneous connective tissue, the so-called epimysium. Together they form the muscle fibers, which are organized in fiber bundles. A muscle contains several fiber bundles. Both the whole muscle and fiber bundles are bounded by connective tissue, which are called epimysium and perimysium respectively. Connective tissue is predominantly made up of collagen. A schematic representation of the hierarchical structure of cooking meat is shown in figure 1.

If the proteins in the intracellular phase denature, part of the intracellu-

lar liquid will be expelled to the extracellular phase. If the collagen of the perimysium and epimysium denatures, the liquid in the extracellular phase will be expelled to the environment. We will assume that both liquid transport processes is instantaneous. Or, in other words the time scale of liquid transport is faster than that of protein denaturation. This assumption holds of course only for thin slices of meat. Moreover, for thicker slices of meat there might even be a significant temperature gradient.

Similar to meat, our model for electrical conductivity will have a hierarchical structure. At the lowest length scale, we have a model for the serum phase. At the next level, we have a model describing the conductivity of the intracellular phase. At the highest level, we describe the conductivity of the complete meat, being a composite with an intracellular and extracellular phase, with the latter having the conductivity of serum.

The model for the serum will build upon the conductivity model for salt solutions. Later, this model will be modified for the presence of soluble proteins. For dilute salt solutions there are fundamental physical models like Debye-Hueckel. The conductivity is linked to the ion charge density and its diffusivity (or rather its inverse the mobility), for which the Stokes-Einstein relation is often used. But, this theory breaks down at higher salt concentrations as found in meat products. Hence, we have to resort to empirical relations (Anderko and Lencka, 1997). Because of the relation between conductivity and ionic mobility, one can state that the temperature dependency is independent of the concentration. Hence, the following decomposition holds: $\sigma_s = \sigma_{s,c}(c)\sigma_{s,T}(T)$, with c the concentration and T temperature(Anderko

and Lencka, 1997).

Similarly, the contributions of soluble proteins depend on their charge and mobility. Proteins are polyelectrolytes, and they can carry charges via (dis)association with protons. However, in meat products the pH≈5.8, which is near the isoelectric point pI≈5.3 (Hamoen et al., 2013). Hence, the charge density of the soluble proteins will be negligible compared to that of salts present in meat. Moreover, due to their size their mobility is also small compared to that of salts. Hence, one can neglect their direct ionic contribution compared to salts, similar to milk (Bazinet et al., 2005). Consequently, the soluble proteins can be viewed effectively as insulators. However, they do have an indirect contribution to the conductivity via two effects: 1) the soluble proteins increase the viscosity of the fluid (Shibata-Ishiwatari et al., 2015), and decrease the mobility of salt ions, and 2) as insulators they occupy a fraction of volume, and influence the overall conductivity of serum similar to composites. Similar arguments hold for the proteins in the muscle fibers, which are quite immobilized too.

The electrical conductivity of composites is described by effective medium theory, as pioneered by Maxwell (Choy, 2015). The effective medium theory can equally be applied to other material properties like thermal conductivity and diffusivity, as these transport phenomena are governed by similar mathematical equations. Maxwells theory only holds for spherical inclusions, but the theory has been extended to arbitrary shape by Torquato and Sen (1990). This theory we have applied successfully to the thermal conductivity of (frozen) meat (van der Sman, 2008). There, we have assumed that meat

protein fibers in muscle meat products can be represented as straight cylinders. For the (electrical) conductivity it is important to know the orientation of the meat fibers with respect to the gradients of the field (temperature or electric potential). In minced meat products or meat emulsions the proteins fibers are randomly oriented, and Maxwells effective medium theory for spherical inclusions can be used.

Effective medium theory does not account for the steric effects of the meat structure on the mobility of ions. This effect has been accounted for in theories for the electrical conductivity of poly-electrolyte gels (Gu et al., 2004). The ion diffusivity depends on the porosity and structure of the gel (Amsden, 1998; Gu et al., 2004; Rossi et al., 2016). Various theories exist, but there is no universally accepted theory for that (Amsden, 1998). The structural dependence is assumed to be dependent on the ratio between mesh size of the gel and the ions radius r_i. We will capture this steric hindrance effect by an empirical prefactor in the equations of effective medium theory.

It is assumed that not all soluble proteins from the intracellular phase will migrate to the extracellular phase. It can happen that they have denatured and aggregated, before the contraction of the connective tissue. Consequently, these aggregates will be immobilized, or they will not be able to pass through the mesh of the connective tissue (endomysium). Hence, we assume that all proteins in the intracellular phase are practically immobilized, and they are all absorbed in the dispersed phase. The continuous phase of the intracellular phase is the salt solution only.

The model for the conductivity of the intracellular phase will be tested for

fast heated meats, where the heating rate is faster than the rate of protein denaturation. Under this condition, we assume that the microstructure of meat does not change, and remains comparable to the structure of post-mortem meat. Post-mortem there is a slight extracellular phase with a volume fraction of about 5% (Offer and Cousins, 1992; Oroszvári et al., 2006), but we will neglect this contribution for fast heated meats. Under this assumption the conductivity of fast heated meat is representative for that of the intracellular phase.

For the conductivity of the whole meat, we will assume that meat consists of an array of cylindrical unit cells, with each unit cell having an extracellular and intracellular phase. The intracellular space is regarded as homogenized phase, that has a conductivity modelled with the above described effective medium theory. At the level of the whole meat we reuse the same effective medium theory, with the intracellular phase as the cylindrical dispersed phase, and the extracellular phase as the continuous phase, with the same conductivity as the exuded serum.

During cooking the volumes of the intracellular and extracellular phases will change due to protein denaturation. We will model explicitly the protein denaturation using the Lumrey-Eyring two-state model, building upon the earlier work of Ishiwatari et al. (2013). That model only considers myosin and actin. However, the model is still useful for our purposes because the denaturation behaviour of collagen of the epimysium and perimysium and actin more or less overlap, i.e. perimysium shrinks at 64^oC (Tornberg, 2005), which is the melting temperature T_m of actin (Ishiwatari et al., 2013). Fur-

thermore, only denaturation of actin and/or myosin leads to expulsion of liquid from the intracellular phase to the extracellular phase. If the connective tissue of the epimysium and perimysium denatures, the serum from the extracellular phase will be expelled out of the meat, and the total volume of intracellular and extracellular phase will decrease.

It is noted that in fish products dielectric loss factor is mainly determined by the ionic conductivity up to moderate radio frequencies (27 MHz) (Wang et al., 2008). It is reasonable to assume this also holds for meat products. Hence, for validation of our model we can also use data from Ohmic heating of meat up to such frequencies.

2.2. Electrical conductivity models

Using data obtained from standard works and literature (Zell et al., 2009), one can show that at constant temperature and in the range of $c < 5\%$ the conductivity can be approximated by a linear function. Hence, we will use the following bilinear function:

$$\sigma_s = \sigma_0 c(1 + \nu T) \tag{1}$$

with σ_s the conductivity of salt, c the salt concentration, and T is the temperature. The other symbols are just parameters, which will be fitted.

The Torquato model applied to the intracellular phase reads:

$$\frac{\sigma_{fib}}{\sigma_s} = f\frac{1 + \delta(1 - \phi_w + Q\phi_w)}{1 + \delta Q\phi_w} \tag{2}$$

σ_{fib} is the total conductivity of the fibrous intracellular phase, σ_s is the conductivity of the salt solution, which follows Eq.(1). $\phi_w = 1 - \phi_p$ is the

volume fraction of water in the intracellular phase. δ is the relative difference between the conductivity of protein fibers and salt solution. As we assume the protein to be insulating, it follows that $\delta = -1$ (Torquato and Sen, 1990). Q is a shape factor, which is $Q = \frac{1}{3}$ for spherical inclusions, $Q = 0$ for parallel to fibers, and $Q = \frac{1}{2}$ perpendicular to fibers (Torquato and Sen, 1990). f is the hindrance factor, accounting for the reduction of ion mobility due to the muscle protein structure (i.e. gel).

We describe the conductivity of the serum in the extracellular phase, $\sigma_{s,ex}$. The serum is a salt solution with soluble sarcoplasmic proteins at a volume fraction of $\phi_{ssp} = 0.08$ (Shibata-Ishiwatari et al., 2015). The enhancement of the viscosity by the soluble proteins is described by the Einstein relation $\eta_{ex} = \eta_w(1 + 2.5\phi_{ssp})$, with η_{ex} the viscosity of the serum, η_w is the viscosity of the salt solution. The increase of viscosity will lead to reduction of the mobility of the salt ions, which is inversely proportional to the viscosity. The soluble proteins act as insulating spheres, which can be captured by the Torquato model, using $Q_{ex} = \frac{1}{3}$. Hence, the conductivity of the serum can be estimated as:

$$\sigma_{s,ex} = \frac{\sigma_s}{1 + 2.5\phi_{ssp}} \frac{1 - \phi_{ssp} - (1 - \phi_{ssp})Q_{ex}}{1 - Q_{ex}(1 - \phi_{ssp})} \tag{3}$$

Subsequently, we apply the Torquato model at the level of the total muscle. The extracellular phase is the continuous phase, and the fibrous intracellular phase is the dispersed phase - whose conductivity is described with Eq.(2). For the conductivity of the total meat σ_{meat} holds:

$$\frac{\sigma_{meat}}{\sigma_{s,ex}} = \frac{1 + \delta_{ex}(1 - \phi_{ex} + Q\phi_{ex})}{1 + \delta_{ex}Q\phi_{ex}} \tag{4}$$

with $\delta_{ex} = (\sigma_{fib} - \sigma_{s,ex})/\sigma_{s,ex}$, the relative difference in conductivity between the fibrous intracellular phase, and the serum in the extracellular phase. Q is the same shape factor as for the intracellular phase. ϕ_{ex} is the volume fraction of the extracellular phase with respect to the whole meat. In a following section, we will compute ϕ_{ex} and ϕ_w as a function of the degree of protein denaturation. But, first the protein denaturation models are discussed.

2.3. Protein denaturation

The model for the denaturation of muscle proteins builds upon the work of Ishiwatari et al. (2013). These authors have considered the denaturation of both myosin and actin only. They have assumed that protein denaturation is irreversible. However, this assumption is not consistent with the notion of water holding of meat. In the recent theories developed for water holding capacity (WHC) we have assumed that it is an equilibrium property (van der Sman, 2012). This means that meat can hold a certain defined amount of water, if it is held at a certain temperature for a long period of time. We have treated WHC within the framework of thermodynamics, which presumes that the protein denaturation is (partly) reversible (van der Sman, 2012). Hence, we will extend the Ishiwatari model with reversibility. Only reversibility of the protein denaturation can explain the thermodynamic property of the water holding capacity of meat. After a very long period (days) of heating at constant temperature, the WHC is still a strong function of temperature (Zielbauer et al., 2016). This implies that at temperatures below 80^oC protein denaturation is only partial, and that it has reached thermodynamic equi-

librium. The partial denaturation follows indeed from DSC measurements (Zielbauer et al., 2016).

The kinetic model of protein denaturation can be made consistent with the framework of thermodynamics, if the denaturation reactions are assumed reversible, similar to the Lumry-Eyring models of protein denaturation (Lumry and Eyring, 1954). Protein denaturation is often compared to melting behaviour of (semi)-crystalline biopolymers, having a defined melting temperature T_m and melting enthalpy ΔH_m. The melting transition takes places over a broad temperature range. We will assume that the reaction constant of the protein denaturation will follow similar temperature dependency as melting crystals.

Below, we will give a general description of protein denaturation, which is assumed to hold also for the meat proteins, myosin and actin. The protein is assumed to have two states: N the native state, and D the denatured state. The corresponding mass balance is as follows:

$$\begin{aligned} dN/dt &= -k_D N + k_N D \\ dD/dt &= +k_D N - k_N D \end{aligned} \tag{5}$$

In equilibrium holds that $dN/dt = dD/dt = 0$. The initial amount of native protein is $N(0) = N_0 = N + D$ and $D(0) = 0$. The fraction denaturated proteins is denoted as $D/N_0 = x$. The equilibrium condition is:

$$dx/dt = -k_D(1 - x) + k_N x = 0 \tag{6}$$

And hence, the equilibrium value of the fraction of denatured proteins is:

$$x_{eq} = \frac{k_D}{k_N + k_D} = \frac{1}{K+1} \tag{7}$$

$K = k_N/k_D$ is the reaction constant, which follows the temperature dependency of melting crystals:

$$K = K_0 \exp(-\Delta G/RT) \tag{8}$$

The change in free energy ΔG is due to melting of crystalline parts:

$$\Delta G = \Delta H_m(1 - T/T_m) \tag{9}$$

k_N is often modelled following the Eyring transition state theory, where it is assumed that an energy barrier with height ΔE must be overcome:

$$k_N = k_{N,0} \exp(-\Delta E/RT) \tag{10}$$

Hence, the denaturation kinetics follows:

$$k_D = k_{N,0} \exp(-\Delta E/RT) \exp(-\Delta G/RT) \tag{11}$$

The above model will be applied to actin and myosin, whose denaturation will be described by the fractions x_{act} and x_{myo}. Below, we describe how the volume fractions ϕ_w and ϕ_{ex} can be related to these numbers.

2.4. Evolution of microstructure as function of protein denaturation

The consequences of muscle protein denaturation is indicated schematically in figure 2. There we have represented the meat with a cylindrical

unit cell, having an extracellular and intracellular phase. The figure shows the sequence of the principal steps in the evolution of the intracellular and extracellular volumes. At low temperatures, the cell volume V_{cell} equals the initial volume V_0. There is no extracellular phase, meaning the total volume equals the cell volume ($V_{tot} = V_{cell}$). Above 40^oC myosin starts to denature, and the cell volume (the intracellular phase) shrinks linear with the fraction of denatured myosin, x_{myo}. The shrinking cells expels liquid to the extracellular phase. The total volume still remains equal to the initial volume $V_{tot} = V_0$. At temperatures above 60^oC actin and collagen of the perimysium and epimysium will denature. The denaturation of actin will have similar effect as the denaturation of myosin: the intracellular phase shrinks linear with the fraction of denatured protein, $x_{myo} + x_{act}$, and the excess liquid is expelled to the extracellular phase. Due to the denaturation of collagen in the connective tissues the total volume will shrink: $V_{tot} < V_0$. The total volume is thought to be linear with the fraction of denatured actin, x_{act}, which is assumed to coincide with the denaturation of collagen in the perimysium and epimysium. At the end of the protein denaturation, $T > 90^oC$, all liquid from the extracellular phase is expelled and the cell volume equals the total volume again, $V_{tot} = V_{cell} = V_e$. The final cell volume V_e follows from the known water holding capacity of fully cooked meat.

From the above assumptions follows the following linear relations between volumes and fractions of denatured proteins:

$$\frac{V_0 - V_{cell}}{V_0 - V_e} = \tfrac{1}{2}(x_{myo} + x_{act})$$

$$\frac{V_0 - V_{tot}}{V_0 - V_e} = x_{act} \tag{12}$$

From the above equations we derive relations for the volume fraction of proteins in the intracellular phase, $\phi_p = 1 - \phi_w$, and the volume fraction of the extracellular phase ϕ_{ex} (relative to the whole meat).

In our earlier paper we have shown that there is quite some universal behaviour regarding water holding capacity (WHC) of meat from different animal sources (van der Sman, 2012). Hence, we will take the values for WHC from there, which are expressed in terms of mass fraction of water y_w, or equivalently the mass fraction of proteins $y_p = 1 - y_w$. The WHC of raw meat is denoted as $y_{p,0}$, and the WHC of fully denatured meat is $y_{p,e}$. Using the mass densities of proteins and water, ρ_w and ρ_p, the initial and final protein volume fraction can be computed:

$$\begin{aligned} \phi_{p,0} &= \frac{y_{p,0}}{(y_{w,0}\rho_p/\rho_w + y_{p,0})} \\ \phi_{p,e} &= \frac{y_{p,e}}{(y_{w,e}\rho_p/\rho_w + y_{p,e})} \end{aligned} \tag{13}$$

Consequently, the instantaneous protein volume fraction in the intracellular phase is given by:

$$\frac{\phi_p}{\phi_{p,0}} = \frac{V_{cell}}{V_0} \tag{14}$$

This value will be substituted in Eq.(2), with use of $\phi_w = 1 - \phi_p$.

The volume fraction of the extracellular phase, relative to the total volume is given by:

$$\phi_{ex} = \frac{V_{tot} - V_{cell}}{V_{tot}} \tag{15}$$

This value will be substituted in Eq.(4).

2.5. Use of the model

In the following we describe the use the complete model for the description of the electrical conductivity of slowly heated meat. Furthermore, several submodels can be validated using literature data for special cases. A visual representation of the various uses of the model is given in figure 3, which can be used as a guide in the following discussion.

The basis of the model is the conductivity of a salt solution, Eq.(1). This equation will be tested for salt concentration up to 5%. We will use this equation for the conductivity of the continuous phase of the intracellular phase, which is modelled using the Torquato model for composites, Eq.(2). This model is also assumed to hold for fast heated meat, whose data is used for validation. Using the shape factor we can acknowledge the orientation of the cylindrical fibers with respect to the electric field. The same model with $Q = \frac{1}{3}$ can be used for minced meat, or meat emulsions, where the proteins are randomly oriented. These meat products can contain also some fat, which can also be viewed as an insulating dispersed phase similar to the proteins.

The protein denaturation is described by the two-state model, Eq.(5). Model parameters will be determined seperately for the main proteins myosin and actin, using literature data on denaturation as measured by DSC.

In slowly heated muscle meat a temporary extracellular phase will form. The intracellular phase is regarded as a homogenized material, whose conductivity is given by Eq.(2). The serum in the extracellular phase is a salt solution with some soluble proteins, whose conductivity is given by Eq.(3).

The total conductivity of muscle meat is again described by the Torquato model, Eq.(4), where the intracellular phase is assumed as a homogenized dispersed phase having a conductivity σ_{fib}, embedded in the serum of the extracellular phase with conductivity $\sigma_{s,ex}$. With shape factor Q we account for the fiber direction with respect to the electric field.

The volume fraction of the extracellular phase ϕ_{ex}, and the volume fraction of water in the intracellular phase ϕ_w are coupled to the amount of protein denaturation via Eqs.(12)-(15).

3. Results

3.1. Conductivity of salt solutions

The data for the electrical conductivity of salt (NaCl) solutions have been obtained from standard works and literature (Zell et al., 2009). At room temperature the conductivity can be fitted with a third order polynomial for concentrations up to c=25% (see figure 4a). However, for the temperature dependency, only data is available for $c = 1.5\%$ and $c = 2.5\%$. In the range of $c < 5\%$ the conductivity as function of concentration can be approximated by a function linear in c. In this concentration range the literature data shows that σ/c versus temperature renders a master curve (see figure 4b). Hence the above decomposition holds, i.e. $\sigma_s = \sigma_{s,c}(c) \times \sigma_{s,T}(T)$. Linear regression shows that the conductivity follows:

$$\sigma_s = c(1.47 + 0.027(T - 25)) \tag{16}$$

with T given in degrees Celsius, and σ_s in S/m.

3.2. Electrical conductivity of fast heated meat

We extend our investigations towards meat products, which are heated fast via Ohmic heating at rates between 10-160^{o}C/min (Zell et al., 2009; Shirsat et al., 2004; Piette et al., 2004; Jin et al., 2015). We assume that at temperatures below 60^{o}C there is no significant change in microstructure due protein denaturation. The experimental data will be compared to the submodel describing the electrical conductivity of the intracellular phase, Eq.(2).

If it is not specified in literature, we will assume that the volume fraction of water in the myofibers ϕ_w can be estimated from the normal mass fraction of water in meat, which is 75% (van der Sman, 2007). Furthermore, for all meat products we assume there is a contribution of salts naturally occurring in meat, on top of the contribution of added salts. The level of salts naturally present in meat is assumed 0.9%, similar to a physiological saline solution (van der Sman and Boer, 2005).

The model contains only one unknown parameter, which is the hindrance factor f. We will estimate that using the data set on the conductivity of Ohmic heated beef (Zell et al., 2009). Its conductivity is measured at two salt concentrations, namely 1% and 2%. The applied heating rate is 40^{o}C/min for unsalted meat, and 80^{o}C/min for salted meat. The data for the lower salt concentration have been used to parameter estimation, and the higher salt concentration is used for validation. Results are shown in figure 5. Parameter estimation using least squares renders $f = 0.67$. The conductivity data for 2% salt for temperatures below 50^{o}C complies with the prediction of our

model using $f = 0.67$. The effect of the fiber direction is also well predicted. Above 50^oC there is less good agreement between model predictions and experimental data for the pork meat with high salt concentration. The above estimated value of the hindrance factor f will be used for the remainder of this paper.

The validity of the model is also tested using the conductivity data of Ohmic heated fish (Jin et al., 2015). The fish conductivity has been measured both perpendicular and parallel to the muscle fibers. The applied heating rate is about 15^oC/min for fish with fibers parallel to the electric field, and 10^oC/min for fish with fibers perpendicular to the electric field. Model predictions and experimental data are compared in figure 6. Again, we obtain a reasonable prediction of the experimental data at temperatures up to 80^oC. Also the difference due to the fiber orientation is captured.

As a last validation we predict the electrical conductivity of Ohmic heated meat emulsions, as measured in (Shirsat et al., 2004; Piette et al., 2004). The applied heating rates are 160^oC/min for meat emulsion without added salt and about 20^oC/min for meat emulsions with added salts. We apply Eq.(2) with $Q = \frac{1}{3}$, due to the random orientation of the muscle fibers. Furthermore, the fat droplets acting as insulators are assumed to be a dispersed phase similar to proteins. The meat emulsions have varied in salt content from 1-5% and in fat content from 5-30%.

The comparison of the model and experimental data is shown figures 7 and 8. The model predicts reasonable well the observed values. For one odd composition the model prediction deviates strongly from the experimental

data, even at room temperature. We attribute that to experimental error, because for the majority of the investigated compositions the model predictions at temperature below 60^oC are well in agreement. Moreover, the meat emulsion with no added salt (thus with total 1% salt) heated at the rate of 160^oC/min (Shirsat et al., 2004) shows very good agreement even upto 80^oC. At this fast heating rates we expect little effects of protein denaturation. At the slower heated emulsion one finds deviations from the predictions at temperatures above 60^oC, where one can expect deviations due to protein denaturation. There is also some shrinkage of meat due to protein denaturation, which can impart the contact of electrodes and meat, and thus also the conductivity measurement.

All-in-all the model predicts well the observed trends for fast-heated meats: 1) the conductivity is about linear for temperatures upto 60^oC, 2) the conductivity increases with the salt concentration, 3) the conductivity lowers with the increase of fat content, 4) the conductivity is higher if the electric field is parallel to the fibers, as opposed to the situation where the electric field in perpendicular to the fibers, and 5) at temperatures above 60^oC there is often some deviation from the linear increase of conductivity with temperature, which is probably due to structural changes induced by protein denaturation. In the next sections, we will investigate the kinetics of protein denaturation, and its consequences for the electric conductivity.

3.3. Denaturation kinetics of meat proteins

In this section we investigate the thermodynamics and kinetics of protein denaturation, using the model described in section 2.4. The values for the parameter characterizing the melting behaviour of myosin and actin are obtained from (Ishiwatari et al., 2013). For myosin it holds $T_{m,myo} = 50^oC$, and $\Delta H_{m,myo} = 241$ kJ/mol, while for actin holds $T_{m,act} = 65^oC$ and $\Delta H_{m,act}$=380 kJ/mol.

First, we check the hypothesis concerning the reversibility of protein denaturation using data of Water Holding Capacity (van der Sman, 2013). We assume that water is equally distributed over myosin and actin, and consequently that the WHC is linear with $x_{eq} = \frac{1}{2}(x_{eq,myo} + x_{eq,act})$, with $x_{eq,i}$ given by Eq.(7-9). The WHC of meat is shown to be quite universal, and we compare x_{eq} with WHC data from (van der Sman, 2013). We have normalized the WHC as:

$$w = \frac{WHC(T) - WHC_{cooked}}{WHC_{raw} - WHC_{cooked}} \tag{17}$$

The WHC changed from WHC_{raw}=79% for raw meat to WHC_{cooked}=45% for cooked meat (van der Sman, 2013).

If the hypothesis concerning reversibility of protein denaturation is true, we expect that $w = x_{eq}$, with x_{eq} computed using the denaturation model using the above parameter values. Both quantities are compared in figure 9. One can observe that the equilibrium value of the protein denaturation x_{eq} nicely follows the trend in w. Hence, we assume our hypothesis of reversibility to be valid.

The model validation for the kinetics of protein denaturation is performed using literature data concerning the peak temperature of myosin and actin denaturation as measured with DSC (Differential Scanning Calorimetry) as a function of scanning rate. If the time scale of heating is faster or comparable to the time scale of protein denaturation the peak temperature shifts up to higher temperatures with increasing scanning rate. For the analysis of the denaturation of myosin and actin we have found the relevant DSC data in refs. (Kijowski and Mast, 1988; Wagner and Anon, 1985; Ishiwatari et al., 2013; Deng et al., 2002).

The literature data we have analysed with the above model. The peak in the DSC trace we have compared to the peak in the protein denaturation rate, dx/dt. Examples of such peaks in denaturation rates are shown in figure 10, as computed with the above model. One can observe that the peak shifts to higher temperature with higher heating rates.

From these traces we have determined how the peak temperatures shift with heating rate, for both myosin and actin. We have matched the model predictions with the experimental observations via tuning the reaction rates k_N. The results of this analysis are presented in figure 11. Observe the large scatter in experimental data, but still there is a clear trend that the peak shifts towards higher temperature with higher heating rates.

The results of the parameter estimation are the following. For both proteins holds that the activation energy is E_a/R_{gas}=5500 K, which is often found for biological processes - as expressed in the rule of van't Hof. At $T = 60^oC$, the reaction rates are $k_N = 5.5 \pm 1.5 \times 10^{-3}\ s^{-1}$ for myosin, and

$k_N = 7.0 \pm 0.9 \times 10^{-3}\ s^{-1}$ for actin. The 80% confidence intervals for the peak temperature are indicated as dashed lines in the graph of figure 11.

In the figure one can observe that the model is following the trend in the literature data, which does have quite a lot of scatter - as is also evident in the large confidence intervals. If one compares the graphs, one can state that the denaturation kinetics of actin and mysosin are very similar. Their differences in denaturation behaviour is only due to differences in their melting temperature and enthalpy, which are really thermodynamic factors.

3.4. Electrical conductivity of meat at specific heating rates

Having a valid model for protein denaturation and for electrical conductivity for fast heated meat (i.e. the intracellular phase) we can perform the analysis for the electrical conductivity of slower heated meat, and faster heated meats above 60 degrees Celsius. Data on electrical conductivity of slower heated muscle meat is obtained from the studies (Brunton et al., 2006; Basaran-Akgul et al., 2008), where the heating rate is $10^oC/min$ or lower. The experimental data is only available for conductivity perpendicular to the meat fiber. Both sets of experimental studies show a significant decrease in conductivity at temperatures above 70^{o}C. Model predictions will be made with the complete model, as explained in section 2.5. Please note, that all required model parameters are already estimated in the previous section. Hence, the presented values are really model predictions.

As an example of how protein denaturation modifies the structure of meat, we show in figure 12 how the volume of the intracellular phase V_{cell}, and the

total of intra- and extracellular phase V_{tot} changes with temperature during slow heating at a rate of dT/dt=10^{o}C/min. The difference between the two volumes is a measure for the relative volume of the extracellular phase. Note, that at the start and at the end of heating the extracellular phase is absent. It is only present when proteins are actually denaturing, which happens in the temperature range of $50 < T < 80^o$C. In this temperature range we expect significant deviations of the electrical conductivity from the behaviour as discussed above in case of fast heating.

The model predictions for slow and fast heated muscle (meat) is given in figure 13, where it is compared to the experimental data. We have computed electrical conductivity for muscle meat (without added salts) using slow and fast heating rates of $10^oC/min$ and $160^oC/min$ respectively.

We observe that the electrical conductivity is linear dependent on temperature for fast heating rates at and above $160^oC/min$, where there is little development of the drip channels. In the figure for the fast heating rate one can observe first a slight increase in the electrical conductivity due to drip channel (extracellular phase) formation at temperatures above 80^oC. At the slower heating rates the model predictions of the electrical conductivity indeed follow the trends shown in the experiments. First, there is a slight increase above the linear increase with temperature (due to onset on drip channel formation), followed by a significant decrease at temperatures above 70^oC, which is due to the disappearance of the drip channels and the densification of the intracellular protein matrix. Also, quantitatively the model predictions are quite comparable to the experimental values obtained at the

slow heating rate.

4. Conclusions

In this paper we have presented a predictive model for the development of electrical conductivity of muscle meat during Ohmic heating. The model computes the conductivity as a function of composition, temperature and microstructure. We have assumed that the muscle meat is composed of protein, water, and salt. Concerning the microstructure, the model takes into account the muscle fiber orientation with respect to the electric field, and the development of drip channels due to protein denaturation. The model includes a description of the protein denaturation kinetics, which has been validated independently using DSC measurements. The degree of protein denaturation has been coupled to the development of drip channels, i.e. the extracellular phase.

If the heating rate is faster than $10^oC/min$, the electrical conductivity is more or less linear with temperature in the range $T < 60^oC$. In this regime the time scale of heat transfer is much faster than that of the protein denaturation, and consequently there is little drip channel formation. The muscle meat behaves as a homogeneous gel, where the polymers are oriented in a defined direction. The proteins act as insulators, and also hinder the mobility of salt ions.

If the heating rate is slower than $15^oC/min$, the electrical conductivity is showing a strong non-linear dependence with temperature. The most striking effect is the strong decrease in conductivity at temperatures above 70^oC. This

non-linear behaviour is explained by the changes in microstructure (i.e. drip channels). At the maximal conductivity, the drip channel volume is maximal, and the collagen in the connective tissue has not shrunken yet. The serum in the drip channels is not hindered in its mobility by a protein matrix as in the intracellular phase, leading to an increase of conductivity above that of the fast heated meat.

The subsequent shrinkage of the collagen of the perimysium and epimysium makes the drip channels to disappear, and the protein matrix densifies even more due to the denaturation of actin. The conductivity is lowered due to the absence of the drip channels, and the densified protein matrix of the intracellular phase (which is due to the loss in Water Holding Capacity). This decrease of conductivity with temperature is also shown for other meat products as in the study on Ohmic heating of thick pieces of minced meat Bozkurt and Icier (2010), which occurs at $T > 65^oC$. At temperatures above 90^oC one can expect a further increase of the conductivity due to increase of the conductivity of the salt solution with temperature.

Take note that the above model presumes immediate loss of extracellular water, where as in large pieces of meat it will take time for the drip to flow through the channels. Hence, for proper modelling of water holding also the kinetics of water loss, as modelled previously (van der Sman, 2007), needs to be taken into account. Such a model can be extended to meat emulsions if water loss is accompanied by fat loss, as observed by Bozkurt and Icier (2010). Such a model for electrical conductivity can well be used in a simulation model for evaluating Ohmic heating for meat products. Be

aware that at slow heating rates there is some degree of protein denaturation, and consequently there is also some shrinkage of the meat. This can lead to poor contact of the meat with the electrodes, and possible dissipation of heat in the fluid in between electrode and meat. Hence, for proper evaluation of Ohmic heating the shrinkage problem has to be taken into account.

Furthermore, the presented model can be a basis for computing the WHC as function of heating rate. From the protein denaturation model follows the distribution of water over intra- and extracellular phase. The water binding in the intracellular phase can be described by the Flory-Rehner theory, as we have applied earlier to muscle meat, vegetables and other food gels (van der Sman, 2007, 2012; van der Sman et al., 2013; Paudel et al., 2015; van der Sman, 2015; Paudel et al., 2016). The water in the extracellular phase is held by capillary pressure, which can be related to the radius of the drip channels. The water in the drip channels is easily drained upon exertion of mechanical force. If the water binding in the drip channels by the capillary pressure can be incorporated in the thermodynamic framework of the Flory-Rehner theory, one can predict how much water can be held under defined mechanical forces.

Acknowledgements

The research is part of the PPS Mild preservation project, which is co-financed by the Top Consortium for Knowledge and Innovation Agri & Food by the Dutch Ministry of Economic Affairs.

B Amsden. Solute diffusion within hydrogels. mechanisms and models. *Macromolecules*, 31(23):8382–8395, 1998.

A Anderko and MM Lencka. Computation of electrical conductivity of multicomponent aqueous systems in wide concentration and temperature ranges. *Industrial & Engineering chemistry research*, 36(5):1932–1943, 1997.

N Basaran-Akgul, P Basaran, and BA Rasco. Effect of temperature (- 5 to 130 c) and fiber direction on the dielectric properties of beef semitendinosus at radio frequency and microwave frequencies. *Journal of Food Science*, 73 (6):E243–E249, 2008.

L Bazinet, F Castaigne, and Y Pouliot. Relative contribution of proteins to conductivity changes in skim milk during chemical acidification. *Applied Engineering in Agriculture*, 21(3):455–464, 2005.

C Bircan and SA Barringer. Determination of protein denaturation of muscle foods using the dielectric properties. *Journal of Food Science*, 67(1):202–205, 2002.

C Bircan, SA Barringer, and ME Mangino. Use of dielectric properties to detect whey protein denaturation. *Journal of microwave power and electromagnetic energy*, 36(3):179–186, 2001.

M Bouhrara, S Clerjon, JL Damez, C Chevarin, S Portanguen, Al Kondjoyan, and JM Bonny. Dynamic mri and thermal simulation to interpret defor-

mation and water transfer in meat during heating. *Journal of agricultural and food chemistry*, 59(4):1229–1235, 2011.

H Bozkurt and F Icier. Electrical conductivity changes of minced beef–fat blends during ohmic cooking. *Journal of Food Engineering*, 96(1):86–92, 2010.

NP Brunton, JG Lyng, L Zhang, and JC Jacquier. The use of dielectric properties and other physical analyses for assessing protein denaturation in beef biceps femoris muscle during cooking from 5 to 85 c. *Meat Science*, 72(2):236–244, 2006.

TC Choy. *Effective medium theory: principles and applications*, volume 165. Oxford University Press, 2015.

JL Damez and S Clerjon. Quantifying and predicting meat and meat products quality attributes using electromagnetic waves: An overview. *Meat science*, 95(4):879–896, 2013.

Y Deng, K Rosenvold, AH Karlsson, P Horn, J Hedegaard, CL Steffensen, and HJ Andersen. Relationship between thermal denaturation of porcine muscle proteins and water-holding capacity. *Journal of Food Science*, 67 (5):1642–1647, 2002.

WY Gu, H Yao, AL Vega, and D Flagler. Diffusivity of ions in agarose gels and intervertebral disc: effect of porosity. *Annals of biomedical Engineering*, 32(12):1710–1717, 2004.

JR Hamoen, HM Vollebregt, and RGM van der Sman. Prediction of the time evolution of ph in meat. *Food chemistry*, 141(3):2363–2372, 2013.

N Ishiwatari, M Fukuoka, and N Sakai. Effect of protein denaturation degree on texture and water state of cooked meat. *Journal of Food Engineering*, 117(3):361–369, 2013.

H Jaeger, A Roth, S Toepfl, T Holzhauser, KH Engel, D Knorr, RF Vogel, N Bandick, S Kulling, and V Heinz. Opinion on the use of ohmic heating for the treatment of foods. *Trends in Food Science & Technology*, 55:84–97, 2016.

Y Jin, YD Cheng, M Fukuoka, and N Sakai. Electrical conductivity of yellowtail (seriola quinqueradiata) fillets during ohmic heating. *Food and Bioprocess Technology*, 8(9):1904–1913, 2015.

N Kaur and AK Singh. Ohmic heating: Concept and applicationsa review. *Critical reviews in Food Science and nutrition*, 56(14):2338–2351, 2016.

JM Kijowski and MG Mast. Thermal properties of proteins in chicken broiler tissues. *Journal of Food Science*, 53(2):363–366, 1988.

A Kondjoyan, S Oillic, S Portanguen, and JB Gros. Combined heat transfer and kinetic models to predict cooking loss during heat treatment of beef meat. *Meat science*, 95(2):336–344, 2013.

R Lumry and H Eyring. Conformation changes of proteins. *The Journal of Physical Chemistry*, 58(2):110–120, 1954.

JG Lyng, BM McKenna, and K Myer. Ohmic pasteurization of meat and meat products. *Handbook of Farm, Dairy and Food Machinery Engineering, 2nd ed., Academic Press, Elsevier Inc., USA*, pages 541–570, 2013.

F Marra. Mathematical model of solid food pasteurization by ohmic heating: Influence of process parameters. *The Scientific World Journal*, 2014, 2014.

BM McKenna, J Lyng, N Brunton, and N Shirsat. Advances in radio frequency and ohmic heating of meats. *Journal of Food Engineering*, 77(2): 215–229, 2006.

G Offer and T Cousins. The mechanism of drip production: formation of two compartments of extracellular space in muscle post mortem. *Journal of the Science of Food and Agriculture*, 58(1):107–116, 1992.

BK Oroszvári, CS Rocha, I Sjöholm, and E Tornberg. Permeability and mass transfer as a function of the cooking temperature during the frying of beefburgers. *Journal of Food Engineering*, 74(1):1–12, 2006.

E Paudel, RM Boom, and RGM van der Sman. Change in water-holding capacity in mushroom with temperature analyzed by flory-rehner theory. *Food and Bioprocess Technology*, 2015. doi: 10.1007/s11947-014-1459-7.

E Paudel, RM Boom, and RGM van der Sman. Effects of porosity and thermal treatment on hydration of mushrooms. *Food and Bioprocess Technology*, 9(3):511–519, 2016.

KL Pearce, K Rosenvold, HJ Andersen, and DL Hopkins. Water distribution and mobility in meat during the conversion of muscle to meat and ageing and the impacts on fresh meat quality attributesa review. *Meat Science*, 89(2):111–124, 2011.

G Piette, ML Buteau, D De Halleux, L Chiu, Y Raymond, HS Ramaswamy, and M Dostie. Ohmic cooking of processed meats and its effects on product quality. *Journal of Food Science*, 69(2):fep71–fep78, 2004.

F Rossi, G Perale, and M Masi. Principles of controlled drug release: A mass transport matter. In *Controlled Drug Delivery Systems*, pages 9–33. Springer, 2016.

N Shibata-Ishiwatari, M Fukuoka, and N Sakai. Changes in the viscosity of expressible water in meat during heating: Description based on the denaturation kinetics of water-soluble proteins. *Food Science and Technology Research*, 21(4):525–530, 2015.

N Shirsat, JG Lyng, NP Brunton, and BM McKenna. Conductivities and ohmic heating of meat emulsion batters. *Journal of Muscle Foods*, 15(2): 121–137, 2004.

E Tornberg. Effects of heat on meat proteins–implications on structure and quality of meat products. *Meat science*, 70(3):493–508, 2005.

S Torquato and AK Sen. Conductivity tensor of anisotropic composite media from the microstructure. *Journal of applied physics*, 67(3):1145–1155, 1990.

683 RGM van der Sman. Moisture transport during cooking of meat: An analysis
684 based on flory–rehner theory. *Meat science*, 76(4):730–738, 2007.

685 RGM van der Sman. Prediction of enthalpy and thermal conductivity of
686 frozen meat and fish products from composition data. *Journal of Food*
687 *Engineering*, 84(3):400–412, 2008.

688 RGM van der Sman. Thermodynamics of meat proteins. *Food Hydrocolloids*,
689 27(2):529–535, 2012.

690 RGM van der Sman. Modeling cooking of chicken meat in industrial tunnel
691 ovens with the flory–rehner theory. *Meat science*, 95(4):940–957, 2013.

692 RGM van der Sman. Hyperelastic models for hydration of cellular tissue.
693 *Soft matter*, 11(38):7579–7591, 2015.

694 RGM van der Sman and E Boer. Predicting the initial freezing point and
695 water activity of meat products from composition data. *Journal of Food*
696 *Engineering*, 66(4):469–475, 2005.

697 RGM van der Sman, E Paudel, A Voda, and S Khalloufi. Hydration prop-
698 erties of vegetable foods explained by flory–rehner theory. *Food Research*
699 *International*, 54(1):804–811, 2013.

700 KS Varghese, MC Pandey, K Radhakrishna, and AS Bawa. Technology,
701 applications and modelling of ohmic heating: a review. *Journal of Food*
702 *Science and technology*, 51(10):2304–2317, 2014.

JR Wagner and MC Anon. Denaturation kinetics of myofibrillar proteins in bovine muscle. *Journal of Food Science*, 50(6):1547–1550, 1985.

Y Wang, J Tang, B Rasco, F Kong, and S Wang. Dielectric properties of salmon fillets as a function of temperature and composition. *Journal of Food Engineering*, 87(2):236–246, 2008.

G Yildiz-Turp, IY Sengun, P Kendirci, and F Icier. Effect of ohmic treatment on quality characteristic of meat: A review. *Meat science*, 93(3):441–448, 2013.

M Zell, JG Lyng, DA Cronin, and DJ Morgan. Ohmic heating of meats: Electrical conductivities of whole meats and processed meat ingredients. *Meat science*, 83(3):563–570, 2009.

BI Zielbauer, J Franz, B Viezens, and TA Vilgis. Physical aspects of meat cooking: Time dependent thermal protein denaturation and water loss. *Food Biophysics*, 11(1):34–42, 2016.

Table 1: List of symbols

Symbol	Description	Unit
f	friction factor	[-]
k	reaction rate	[1/s]
t	time	[s]
x	mole fraction	[-]
y	mass fraction	[-]
D	amount of denatured proteins	[mol/m^3]
E	activation energy	[J/mol]
G	free energy	[J/mol]
H	enthalpy	[J/mol]
K	reaction constant	[-]
N	amount of native proteins	[mol/m^3]
Q	shape factor	[-]
R	gas constant	[J/mol.K]
T	Temperature	[K]
V	volume	[m^3]
δ	relative difference in conductivity	[-]
η	viscosity	[Pa.s]
ϕ	volume fraction	[-]
ρ	density	[kg/m^3]
σ	conductivity	[S/m]

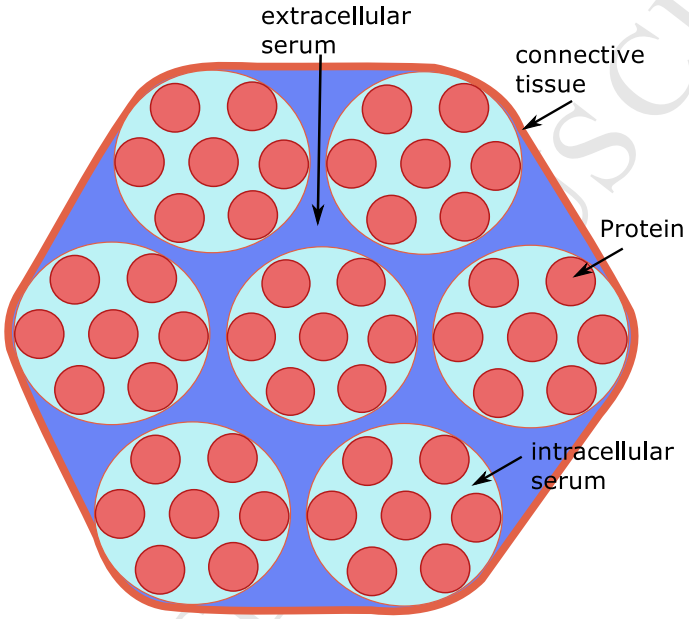

Figure 1: The hierarchical composite structure of cooking meat. At the largest length scale we distinguish the extracellular and intracellular phases. The intracellular phase is bounded by connective tissue, and its internal structure is assumed to consist of protein fibers (cylinders) embedded in serum. The extracellular phase contains the same serum, which is a mixture of water, salt and soluble proteins.

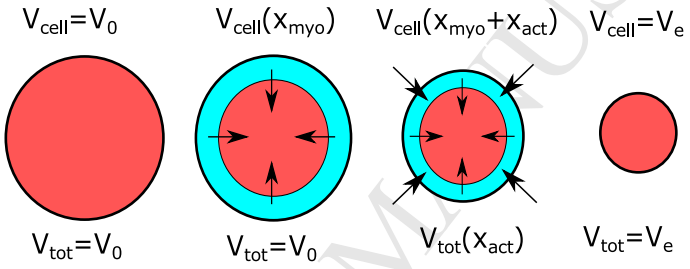

Figure 2: Schematic representation of the development of the microstructure of meat, where we have depicted the volume (cross sections) of intracellular phase (V_{cell} in pink) and extracellular phase (in blue). The total volume V_{tot} is the sum of intra- and extracellular phase. The volumes evolves as a function of the fraction of denatured proteins x_{act} and x_{myo}.

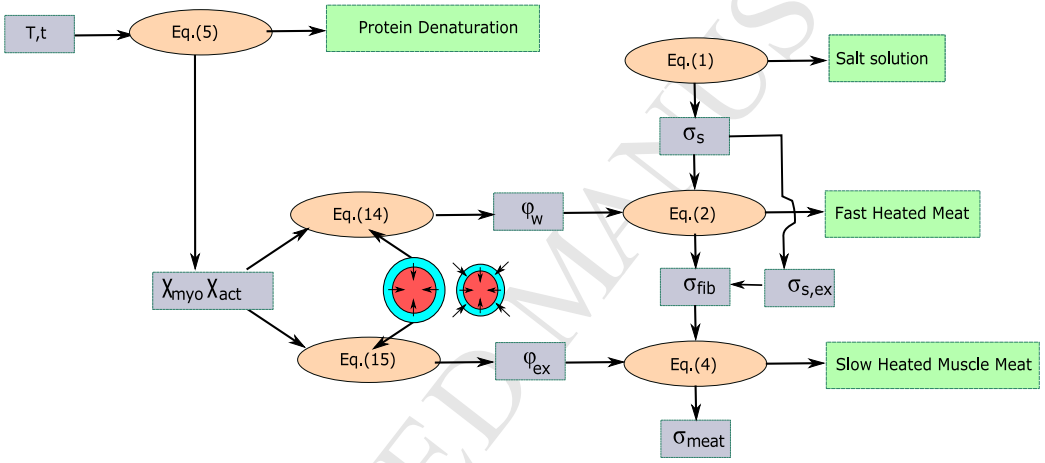

Figure 3: A flowchart showing how the equations of the model connect to each other, and how the submodels can be used for different problems as shown in the green boxes. Inputs and outputs to the equations are shown as blue boxes.

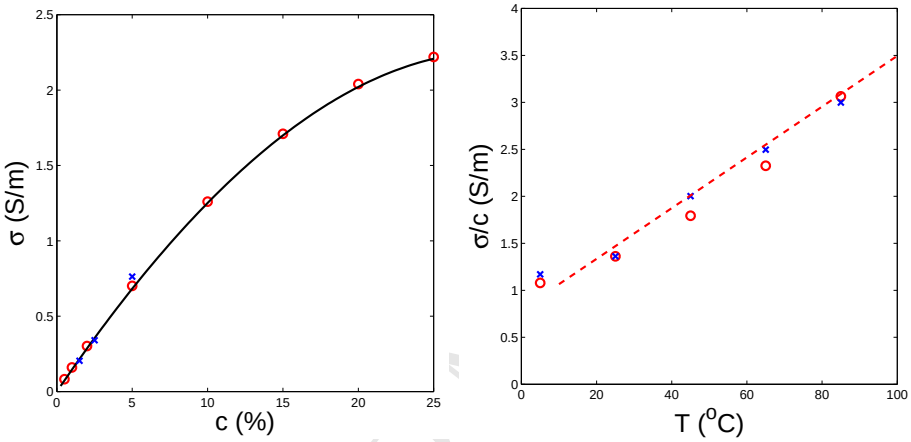

Figure 4: a) Electrical conductivity σ of salt solution at room temperature as function of concentration (mass fraction) c. Data are obtained from the CRC Handbook of Chemistry and Physics and Zell (Zell et al., 2009) (symbols), and fitted by a third order polynomial (solid line). b) Electrical conductivity (normalized with concentration) σ/c of salt solution as function temperature for c=1.5 and 2.5%, with data obtained from (Zell et al., 2009). The dashed line is obtained via linear regression.

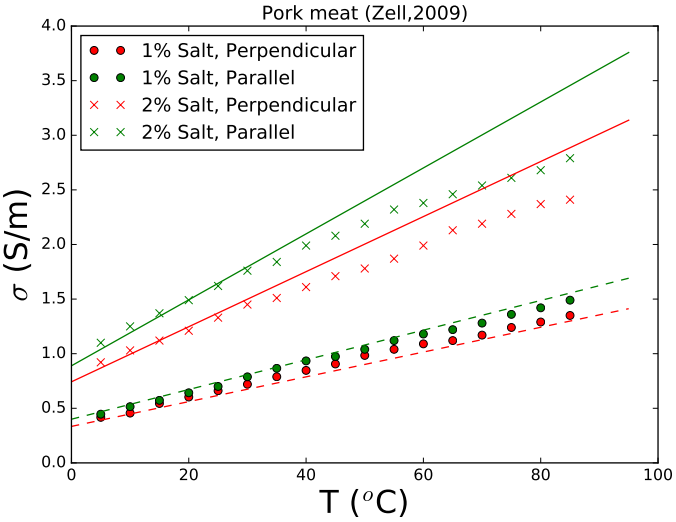

Figure 5: Electrical conductivity of beef, as measured by Zell (Zell et al., 2009), and compared to model calculations (lines). Model has been fitted to low salt meat, using Eq.(2), and the data on high salt meat is used for validation.

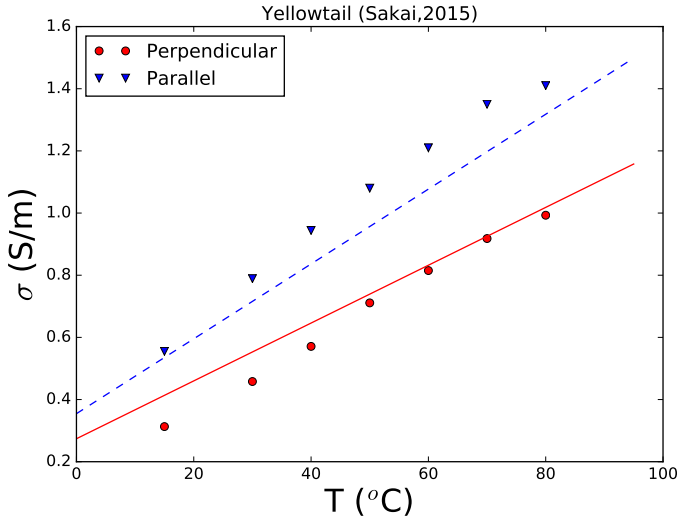

Figure 6: Predictions of electrical conductivity (lines) versus data on Yellowtail fish (Jin et al., 2015) using Eq.(2).

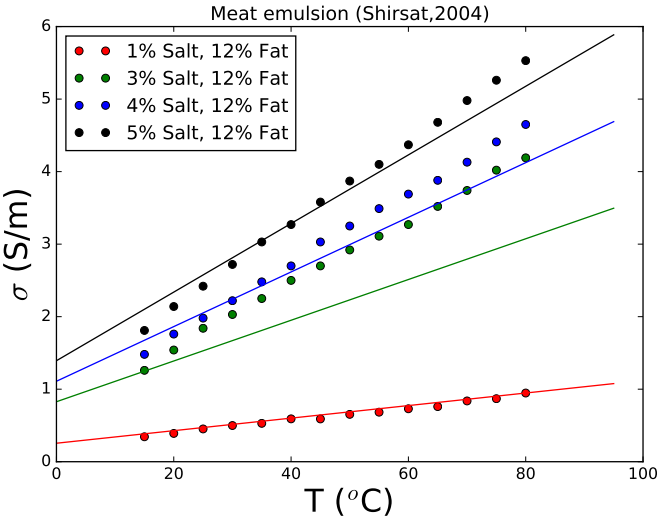

Figure 7: Predictions of electrical conductivity (lines) versus data on meat emulsions (Shirsat et al., 2004) using Eq.(2).

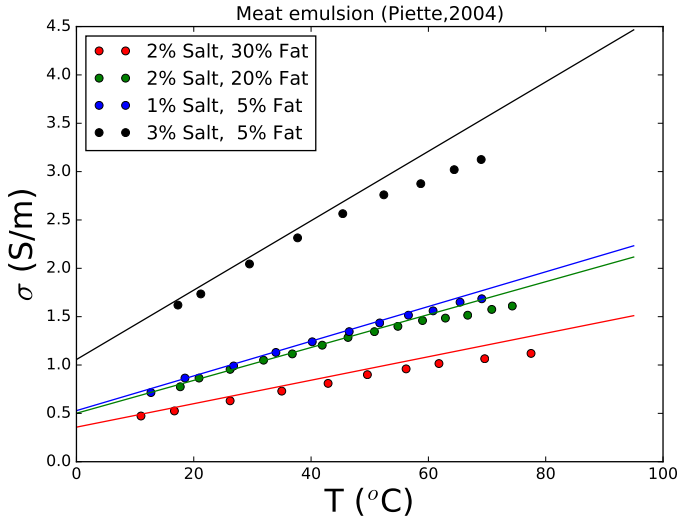

Figure 8: Predictions of electrical conductivity (lines) versus data on meat emulsions (Piette et al., 2004) using Eq.(2).

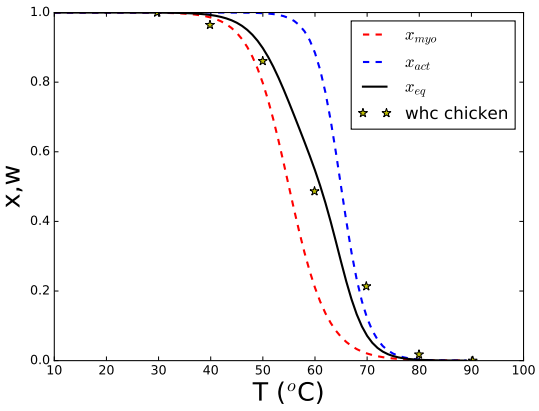

Figure 9: Theoretical fraction of native protein versus temperature (solid line), compared to the dimensionless WHC of chicken meat (symbols), with data obtained from (van der Sman, 2013). The dashed lines indicate the individual contributions of myosin (red) and actin (blue) as computed from the steady state solutions of Eqs.(5).

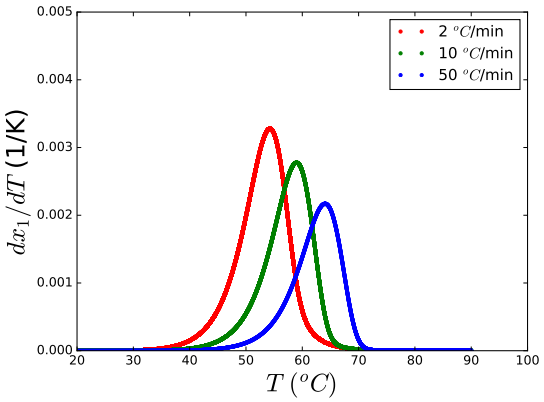

Figure 10: Peaks in denaturation rate of myosin dx_{myo}/dt as function of heating rate dT/dt. For clarity of presentation of data the denaturation rate is rescaled with the heating rate, i.e. $dx_{myo}/dT = (dx_{myo}/dt) \times (dT/dt)^{-1}$. Traces are shown for three heating rates. DSC traces are proportional to dx_{myo}/dt due to absorbance of latent heat.

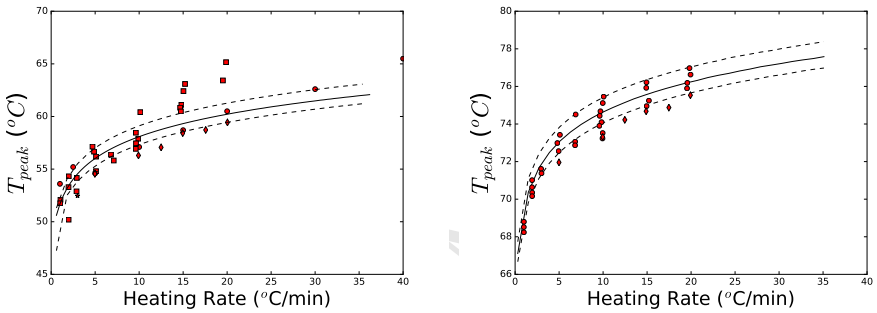

Figure 11: Shift of peak temperature T_{peak} in the DSC scan as function of heating rate, analysed for myosin (left pane), and actin (right pane). Symbols represent data from different literature sources, and -the solid line represent the fitted model, Eqs.(5), with the dashed lines indicating the 80% confidence intervals.

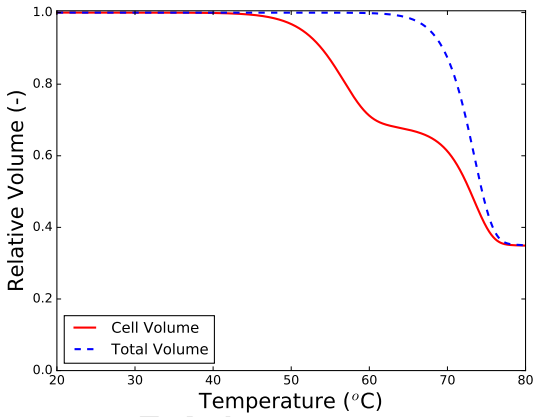

Figure 12: Evolution of the relative volume of intracellular phase, V_{cell}, and total volume of intra- and extracellular phase, V_{tot}, as function of temperature during heating at a rate of 10^{o}C per minute. The initial cell volume is taken as a reference.

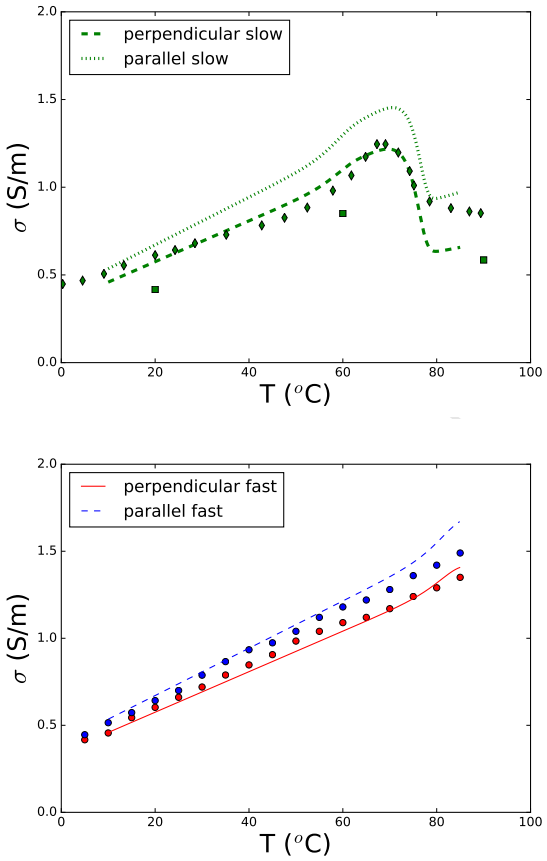

Figure 13: Conductivity of lean meat in perpendicular and parallel direction, following experimental data of (Zell et al., 2009) (for fast heating) and (Brunton et al., 2006; Basaran-Akgul et al., 2008) (for slow heating). Slow heating are indicated with green lines and symbols, and fast heating with red and blue symbols or lines. The lines are model predictions using the complete model, including protein denaturation as function of heating rate. The shown fast heating curves are given for $160^oC/min$, while the slow heating curve is computed for $dT/dt = 10^oC/min$.

- Model predicts electrical conductivity of meat as function of composition and heating rate
- Model considers effect of structural changes induced by protein denaturation
- Slow to moderate heated meat show a drop in conductivity at T>70 degrees
- A submodel predicts meat protein denaturation kinetics